AD-A123 237 NUMERICAL STUDY OF PHASE CONJUGATION IN STIMULATED BRILLOUIN SCATTERING FROM AN OPTICAL WAVEGUIDE(U) NAVAL RESEARCH LAB WASHINGTON DC R H LEHMBERG 30 DEC 82 1/1

UNCLASSIFIED NRL-MR-4985 F/G 20/6 NL

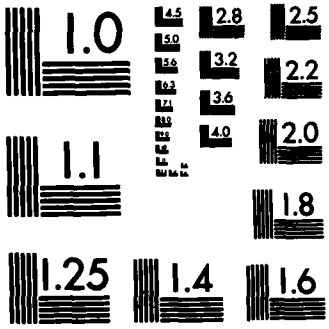

NRL Memorandum Report 4985

Numerical Study of Phase Conjugation in Stimulated Brillouin Scattering from an Optical Waveguide

R. H. LEHMBERG

Laser Plasma Branch
Plasma Physics Division

December 30, 1982

NAVAL RESEARCH LABORATORY
Washington, D.C.

SECURITY CLASSIFICATION OF THIS PAGE (When Data Entered)

REPORT DOCUMENTATION PAGE		READ INSTRUCTIONS BEFORE COMPLETING FORM
1. REPORT NUMBER NRL Memorandum Report 4985	2. GOVT ACCESSION NO. AD-A123237	3. RECIPIENT'S CATALOG NUMBER
4. TITLE (and Subtitle) NUMERICAL STUDY OF PHASE CONJUGATION IN STIMULATED BRILLOUIN SCATTERING FROM AN OPTICAL WAVEGUIDE		5. TYPE OF REPORT & PERIOD COVERED 6. PERFORMING ORG. REPORT NUMBER
7. AUTHOR(s) R. H. Lehmberg		8. CONTRACT OR GRANT NUMBER(s)
9. PERFORMING ORGANIZATION NAME AND ADDRESS U.S. Naval Research Laboratory Washington, DC 20375		10. PROGRAM ELEMENT, PROJECT, TASK AREA & WORK UNIT NUMBERS DOE AI08-79DP 40092(172) 47-0859-0-2
11. CONTROLLING OFFICE NAME AND ADDRESS U.S. Department of Energy Washington, DC 20545		12. REPORT DATE December 30, 1982 13. NUMBER OF PAGES 26
14. MONITORING AGENCY NAME & ADDRESS(if different from Controlling Office)		15. SECURITY CLASS. (of this report) UNCLASSIFIED 15a. DECLASSIFICATION DOWNGRADING SCHEDULE

16. DISTRIBUTION STATEMENT (of this Report)

Approved for public release; distribution unlimited.

17. DISTRIBUTION STATEMENT (of the abstract entered in Block 20, if different from Report)

18. SUPPLEMENTARY NOTES

19. KEY WORDS (Continue on reverse side if necessary and identify by block number)

Wavefront conjugation fidelity
Aberration compensation
Stimulated scattering
Optical waveguide
Pump depletion

20. ABSTRACT (Continue on reverse side if necessary and identify by block number)

Phase conjugation in stimulated Brillouin scattering (SBS) from an optical waveguide is studied numerically, using a Cartesian two dimensional propagation code (BOUNCE) that includes pump depletion. The simulations show that light scattered back through a phase aberrator produces a far field profile closely matching that of the incident beam; however, the near field intensity exhibits large and rapid spatial inhomogeneities across the entire aberrator, even for conjugation fidelities H as high as 98%. This effect can be only partially removed by spatial filtering techniques. The dependence of H upon SBS gain, scattering length L, and the average intensity $\bar{I}$ and
(Continued)

DD FORM 1 JAN 73 1473 EDITION OF 1 NOV 65 IS OBSOLETE
S/N 0102-014-6601

SECURITY CLASSIFICATION OF THIS PAGE (When Data Entered)

20. ABSTRACT (Continued)

angular divergence θ_D of the pump beam is first studied in the low reflectivity regime (i.e., ignoring pump depletion). For amplitude gains $\gtrsim e^{10}$, H decreases monotonically with the factor I/θ_D due to a small scale intensity pulling effect. This result appears to be independent of whether θ_D arises entirely from the aberrator, or from a combination of the aberrator plus curvature introduced by a lens. In all cases, pump depletion is found to enhance the fidelity by inhibiting the small scale pulling effect. Under appropriate conditions, this can actually reverse the intensity dependence of H seen in the absence of pump depletion.

CONTENTS

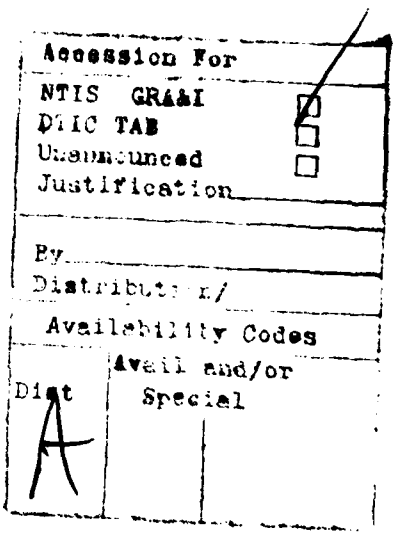

NUMERICAL STUDY OF PHASE CONJUGATION IN STIMULATED BRILLOUIN SCATTERING FROM AN OPTICAL WAVEGUIDE

I. INTRODUCTION

Optical wavefront conjugation in stimulated backscatter has been the subject of extensive experimental and theoretical investigation over the last ten years.[1] Nevertheless, there remain significant gaps in the quantitative understanding of this phenomenon. Analytic theories[2-10] generally agree that it occurs because the component of backscattered light conjugate to a spatially inhomogeneous pump wave will grow at approximately twice the rate of any random modes that are orthogonal to it, and should presumably dominate at sufficiently high gain. They disagree, however, on the question of why some of the backscatter remains unconjugated, even in the high gain regime where the conjugate fraction or fidelity H should approach unity. It is an important question because even a small residue of unconjugated light (e.g. $1 - H \sim 1\%$) can cause serious beam distortion in the near field of the aberator. Zel'dovich[4,5] links this residue to small scale intensity "pulling" by the inhomogeneous pump beam, and predicts that $1 - H$ should increase with the factor $\bar{I}/\theta_D^2$, where $\bar{I}$ is the average intensity and θ_D is the angular divergence of the pump light. However, since the analysis is based on plane wave expansions, it may be inaccurate for describing waveguides. Hellwarth[6] uses the correct waveguide modes, but ignores the terms responsible for the pulling effect. He predicts that under high gain conditions, the fidelity should depend upon the distribution of pump power among the modes (i.e. upon the detailed spatial characteristics of the aberration), but not upon $\bar{I}$. With the exception of Ref. (10), none of these theories includes pump depletion, which becomes important when the backscatter is significantly above threshold. The main result in Ref. (10) is that pump depletion will drastically limit the allowable gain, and hence the conjugation fidelity, if the initial backward propagating noise level is too high. This condition is not applicable to the operating regime of interest here.

In a recent paper,[11] we described a numerical study of wavefront conjugation in stimulated Brillouin scattering (SBS), using a steady state 2D propagation code (BOUNCE) that includes pump depletion. These calculations simulated both aberration correction[12-21] and image replication[22-24] experiments, but they were restricted to the case of a beam focused into a medium unbounded in the transverse direction. The present work examines SBS in a multimode optical waveguide, and studies the parameters that affect the wavefront conjugation fidelity. The key results are summarized below.

(i) The waveguide was able to produce significantly higher fidelities ($H \leqslant 98\%$) than the focused configuration ($H \leqslant 88\%$), in agreement with several experimental studies.[15-19] This improvement occurs because waveguides can avoid the deleterious spatial gain narrowing effects that invariably accompany Gaussian-like pump beam profiles near focus.[8,9,11,25]

(ii) The simulations show that the light scattered back through the phase aberrator exhibits a far field intensity profile closely matching that of the unaberrated incident beam, as seen in experiments,[12-21] while the unconjugated portion appears mainly as low level hash distributed over large angles outside this profile. However, the near field intensity exhibited

Manuscript approved October 22, 1982.

large and rapid spatial inhomogeneities across the entire aberrator in all cases, even when the phase remained uniform to within $\lambda/15$, and the fidelity was 98%. Similar results were found in the previous work.[11] An attempt was made to remove the inhomogeneities by a spatial filtering technique, but this was only partially successful.

(iii) In the absence of pump depletion, the fidelity was found to increase with the average pump intensity for amplitude gains up to around e^{10}, then decrease slowly and monotonically with higher intensity. The low intensity behavior agrees with the usual mode theory,[2-7] which attributes SBS wavefront conjugation to the higher gain experienced by the conjugate wave. At high intensity, the beam profiles clearly show a small scale pulling effect, in qualitative agreement with Zel'dovich;[4,5] however, the detailed parameter study presented here suggests that H varies as $\theta_D/\bar{I}$, rather than the $\theta_D^2/\bar{I}$ predicted in Refs. (4) and (5). A heuristic argument linking this to the discrete nature of the waveguide modes is presented in Sec. V. All of these results appear to be independent of whether θ_D arises entirely from an aberrator, or from a combination of the aberrator plus phase curvature introduced by a lens. This explains why it has been possible to achieve high conjugation fidelities in a waveguide with only a moderately aberrated (or even unaberrated) pump beam.[16]

(iv) In all of the cases studied, pump depletion significantly enhanced the fidelity of the wavefront conjugation by inhibiting the small scale pulling effect. A similar result was found in the focused configuration.[11] If one chooses conditions such that pump depletion starts to become significant at gains around e^{10}, then the fidelity continues to increase with the incident intensity, rather than decreasing as in the cases described above. This result is in good qualitative agreement with the experiments of Mays and Lysiak.[19]

Section II gives a brief description of the nonlinear propagation code, and defines the quantities that are calculated. Section III describes the parameter study in the low reflectivity limit, while Sec. IV looks at the effects of pump depletion. These results are summarized and discussed in Sec. V.

II. THEORY AND CODE DESCRIPTION

Under steady state conditions, the complex pump and SBS backscatter amplitudes $E_L(x, z)$ and $E_S(x, z)$ satisfy the parabolic equations

$$\left(\frac{\partial}{\partial z} + \frac{i}{2k}\frac{\partial^2}{\partial x^2}\right)E_L = \frac{1}{2}g|E_S|^2E_L \tag{1a}$$

$$\left(\frac{\partial}{\partial z} - \frac{i}{2k}\frac{\partial^2}{\partial x^2}\right)E_S = \frac{1}{2}g|E_L|^2E_S \tag{1b}$$

in a two dimensional cartesian geometry. Here, $k = 2\pi n/\lambda$ is the magnitude of the propagation vectors (assumed equal in this paper), x is the transverse coordinate, and g is the coupling constant of the Brillouin medium, which is contained within a region $z_1 \leqslant z \leqslant z_2$. For simplicity, we will take $n \equiv 1$, and ignore refraction in this paper. BOUNCE solves Eqs. (1a,b), assuming an aberrated pump wave $E_L(x, z_2)$ is incident at z_2, while the backscatter grows from a small counterpropagating noise wave $E_S(x, z_1)$ introduced at z_1. (E.g., see Figs. 2 and 8.)

Since E_L and E_S are specified on opposite ends of the medium, and neither steady state solution is known within that medium at the outset, the inclusion of pump depletion is a nontrivial problem. One must know $E_S(x, z)$ in order to calculate $E_L(x, z)$, and vice versa. The brute force solution would be to simply integrate the time dependent equations over many optical transits through the medium until

steady state is finally attained. The approach followed here is an iteration procedure, which is significantly faster. Basically, it starts with an undepleted pump wave $E_L^{(1)}(x, z)$, calculates the resultant backscatter $E_S^{(1)}(x, z)$ throughout the medium, then alternately recalculates these waves until the solutions converge to self consistency. A detailed description of the techniques used to effect this convergence is given in Ref. (11).

In the previous work, all of the beam profiles were assumed to be contained entirely within the transverse region $-W/2 \leqslant x \leqslant +W/2$, taking care to ensure that empty zones were maintained around $\pm W/2$ to simulate propagation in an unbounded medium. The calculations were then performed by a split operator technique,[26] which expanded the field amplitudes using the conventional discrete Fourier transform (DFT) with N transverse points:

$$E(J) = \sum_{K=0}^{N-1} \tilde{E}(K) \exp(i2\pi JK/N) \tag{2a}$$

$$x(J) = (W/N)J - W/2, \quad J = 0, 1, \ldots, N-1 \tag{2b}$$

This expansion has periodic boundary conditions; hence, if a wave were allowed to propagate to one edge (e.g., $+W/2$) it would re-enter from the opposite side (e.g., $-W/2$) as illustrated in Figs. (1a-c).

In this paper, we have simulated propagation in an optical waveguide of width W, where the field amplitudes satisfy the boundary conditions

$$E_{L,S}(W/2, z) = E_{L,S}(-W/2, z) = 0 \tag{3}$$

in all cases; hence, waves will reflect from the boundaries, as illustrated in Figs. (1d-f). This can be accomplished by replacing the usual DFT by a waveguide mode expansion

$$E(J) = \sum_{K=1}^{N-1} \tilde{E}(K)\sin(\pi JK/N), \quad J = 0, 1 \ldots, N-1, \tag{4}$$

which automatically satisfies (3). In the simulations presented here, we followed an equivalent approach, which uses the conventional DFT with $2N$ points. The additional N points $N, N+1, \ldots, 2N-1$ describe the propagation of an external "image" field that satisfies

$$E'(2N-I) = -E(I), \quad I = 1, 2, \ldots, N-1, \tag{5a}$$

$$E'(N) = E(0) = 0. \tag{5b}$$

If the conventional DFT (with $2N$ points) is applied to these combined waves, it will populate only the desired waveguide modes $\sin(\pi JK/N)$.

The accuracy of the modified propagation code was checked in the following ways:

(i) Reruns of some of the earlier simulations, in which the beams remained isolated from $\pm W/2$, were found to give identical results.

(ii) To test free propagation within the waveguide, the numerical results were compared to an analytic calculation (based on multiple images) for the case where an unaberrated cylindrically diverging wave was introduced at the entrance plane. The agreement was excellent.

(iii) If pump depletion is ignored, the total number of points ordinarily used in the calculation (256×601) can be doubled, thus allowing a finer grid in either x or z. When several of the simulations were rerun with these finer grids, the agreement was in all cases better than 1% for the calculated values of H.

The code evaluates several important parameters in addition to the usual pump and backscatter beam profiles. These include the power gain G and total reflectivity R:

$$G \equiv P_S(z_2)/P_S(z_1), \qquad R \equiv P_S(z_2)/P_L(z_2), \tag{6a,b}$$

where

$$P_{L,S}(z) \equiv \int_{-W/2}^{W/2} |E_{L,S}(x, z)|^2 \, dx \tag{7}$$

is proportional to the total pump or backscatter power, assuming unit width along the $\hat{y}$ direction. From Eqs. (1a,b) and (3), one can readily derive the Manley-Rowe relation

$$P_L(z) - P_S(z) = \text{constant} \tag{8}$$

for $\omega_S = \omega_L$. The code also calculates the phase conjugate fidelity defined by the normalized correlation function

$$H(z) \equiv \frac{1}{P_L(z)P_S(z)} \left| \int_{-W/2}^{W/2} E_L(x, z) E_S(x, z) \, dx \right|^2. \tag{9}$$

(Note that $H = 1$ in the case of perfect conjugation $E_S \propto E_L^*$). According to Eqs. (1a,b) and (3), H remains constant when $g = 0$; thus $H = H(z_2)$ at all points beyond z_2.

III. LOW REFLECTIVITY LIMIT

This section will deal with the case where the reflectivity is low enough that pump depletion can be ignored, and thus the pump power P_L will be constant along z.

A. Aberrated Plane Wave

In order to obtain a direct comparison with analytic theories, we first consider the "pure" case where the angular beam divergence θ_D arises only from the aberrator ($\theta_D = \theta_A$), as shown in Fig. 2. A uniform plane wave of $\lambda = 694$ μm traverses a hard aperture of width $W = 2$ mm followed by aberrator A, which imposes a random phase modulation and concomitant far field angular divergence $\theta_A = 20$ mrad (full $1/e$ width), as shown in Fig. 3. The aberrated beam ($\sim$60 $\times$ diffraction limited) then immediately enters the optical waveguide, also of width W.

In all of the simulations presented here, the beam was allowed to propagate 20 cm into the waveguide before entering the scattering medium z_2. This was done in order to ensure a complete mixing of radiation from different parts of the aberrator, so that pronounced intensity (as well as phase) inhomogeneities were present within the entire gain length L; again for purposes of comparison with the analytic theories. In spite of these small scale inhomogeneities, the intensity will remain statistically uniform across the waveguide. This is in contrast to the focused configuration,[11] where the envelope of the intensity profile was typically Gaussian-like. Test runs, in which the free propagation distance was eliminated, yielded similar results, but there was more statistical spread in the data with different members of the aberrator ensemble (i.e., different statistical realizations).

The noise source at z_1 was modelled by a random complex field $E_S(x, z_1)$ of 100 mrad angular divergence, giving initial pump-noise correlations $H_1 = H(z_1)$ typically in the range 0.001 to 0.01. However, the wavefront conjugation of the backscatter was found to be generally insensitive to the statistical properties of the noise source (including even a coherent source) as long as the gain was high enough and H_1 remained small.

Referring now to the lower left hand corner of Fig. 2, one sees that as $E_S(x, z)$ grows and propagates toward z_2, it develops an intensity distribution with small scale inhomogeneities similar to those of $|E_L(x, z)|^2$, giving a fidelity $H = 93\%$. From z_2, the backscatter retraces the pump beam path through the aberrator to produce the near and far field intensity profiles shown on the right hand side of Fig. 2. The phase compensation is evident in the far field, where the backscatter exhibits a strong central spike (of width $2\lambda/W$) and nearby sidelobes almost identical to the $\mathrm{sinc}(x)$ angular spectrum of

the unaberrated incident beam. The ~7% unconjugated component appears mainly as low level background hash extending well beyond this central structure; hence, expression (9) gives

$$1 - H \simeq \frac{\text{background hash}}{\text{total backscatter power}}. \tag{10}$$

For example, if the integrals in expression (9) were evaluated only over the central spike and first three sidelobes, H would jump to 99.3%. Although the peak levels of the background are typically less than 1% of the on-axis intensity, they are still significantly larger than the experimentally observed values.[15–19] This stems from the fact that the hash is confined to only one transverse dimension; i.e., it lacks the usual geometrical weighting factor that would require lower levels in the analogous two-dimensional "halo" in order to satisfy expression (10).

In the near field of the aberrator, the conjugated and unconjugated components become mixed, resulting in serious degradation of the entire profile. This behavior, which was found in all cases both here and in the focused configuration,[11] has gone largely unnoticed in the aberration correction experiments, since these normally record only far field intensities. It will be discussed in greater detail in Sec. V.

Although the analytic theories[2–6] disagree significantly on some issues, they do agree on the primary mechanism that leads to wavefront conjugation; i.e., that the component of the backscatter radiation proportional to $E_L^*(x, z)$ grows at approximately twice the rate of the non-conjugated modes. Since the conjugate field $E_L^*(x, z)$ satisfies the equation

$$\left[\frac{\partial}{\partial z} - \frac{i}{2k}\frac{\partial^2}{\partial x^2}\right] E_L^*(x, z) = 0 \tag{11}$$

in the absence of pump depletion, the lowest order solution of Eq. (1b) can be written in the mode approximation[1–6, 12]

$$E_S(x, z) = C\, E_L^*(x, z) \exp\left[\frac{1}{2}\sigma g \bar{I}(z - z_1)\right] + E_{NC}(x, z) \exp\left[\frac{1}{2} g\, \bar{I}(z - z_1)\right], \tag{12}$$

where C is a constant, $\bar{I} = P_L/W$ is the average pump intensity, and $E_{NC}(x, z)$ is a sum over modes of Eq. (11) that are orthogonal to $E_L^*(x, z)$:

$$\int_{-W/2}^{W/2} E_L(x, z)\, E_{NC}(x, z)\, dx = 0. \tag{13}$$

The theory then predicts that $\sigma = 2$; hence, the first term of (12) will eventually predominate if $g\bar{I}(z - z_1)$ becomes large enough, even though most of the Stokes energy at z_1 resides in the second term. Physically, the condition $\sigma > 1$ is linked to the multimode intensity structure of the pump beam.[12]

One can relate this theory to the numerical calculations by substituting (12) into expression (9), and using (13) to obtain

$$H_1\, P_S(z_1) = |C|^2 P_L \tag{14a}$$

$$H\, P_S(z_2) = |C|^2 P_L \exp(\sigma g \bar{I} L), \tag{14b}$$

where $H_1 = H(z_1)$, $H = H(z_2)$, and $L = z_2 - z_1$. Definition (6a) then yields

$$\sigma = \frac{\ln(GH/H_1)}{g\bar{I}L}. \tag{15}$$

The numerical calculations performed here found $1.95 \leqslant \sigma \leqslant 2.4$, in approximate agreement with mode theory and recent measurements.[20] Surprisingly, the largest values of σ occurred at low fidelities. This is because the large σ and reduction of H are caused by the same intensity pulling effect, which will be discussed in greater detail below.

A more revealing measure of the limitations of the mode approximation is provided by the ratio ρ of output power in the conjugated and unconjugated components of (12):

$$\rho \equiv \frac{|C|^2 P_L \exp(\sigma g \bar{I} L)}{P_{NC} \exp(g \bar{I} L)}, \tag{16}$$

where

$$P_{NC} \equiv \int_{-W/2}^{W/2} |E_{NC}(x, z_1)|^2 \, dx. \tag{17}$$

To rewrite (16) in terms of the calculated quantities, we first substitute (12) into (7) and use (14a) to obtain

$$P_{NC} = P_S(z_1) - |C|^2 P_L = (1 - H_1) P_S(z_1) \simeq P_S(z_1); \tag{18}$$

then combine this result with (14b) and (16):

$$\rho = GH/\exp(g \bar{I} L). \tag{19}$$

Figure 4 shows a plot of $ln\rho$ and the fidelity H as functions of the average gain increment $g\bar{I}L$, using the same 20 mrad aberrator and 75 cm length used in Fig. 2. At low gains, the fidelity improves with $g\bar{I}L$, as one would expect, since ρ is also increasing. With further increase of $g\bar{I}L$, however, H goes through a broad maximum, then slowly declines instead of approaching unity for $ln\rho \gg 1$, as Eq. (12) would predict. Similar behavior was observed with other aberrators and waveguide lengths, with the maximum generally occurring in the range $9 \leqslant G\bar{I}_{max}L \leqslant 11$. (As expected, the larger values of $\bar{I}_{max}$ usually occurred in cases where the initial correlation H_1 was smaller.) This behavior occurs because the inhomogeneous pump beam tends to "pull" a disproportionate amount of the backscattered power into the most intense spikes,[4,5] as seen in the z_2 plots in Figs. 2 and 5. It is therefore a small scale analog of the spatial gain narrowing effect seen in the focused configuration.[11] Since the pulling tendency arises from the exponential nature of the gain term in Eq. (1b), and is counteracted only by the diffraction term, it is expected to become more evident as the gain e-folding length/diffraction length ratio $k\theta_D^2/g\bar{I} = kL\theta_D^2/g\bar{I}L$ decreases. This is illustrated qualitatively by comparing Figs. 2 and 5, which use the same 20 mrad aberrator and approximately the same gain exponent $g\bar{I}L$, but differ by a factor of 3.75 in length.

Zel'dovich and coworkers[4,5] have attempted to treat the pulling effect quantitatively, using a perturbation analysis with the mode approximation as zeroth order. They found that H depends only on the single parameter $k\theta_D^2/g\bar{I}$, approaching unity asymptotically for $k\theta_D^2/g\bar{I} \gg 1$. Here, the 2D version of this theory[5] is compared to the numerical calculations from BOUNCE, using different values of L and θ_D. For each value of L and θ_D, calculations were performed on five different members of the aberrator ensemble, in order to ensure an adequate statistical sampling. Following Zel'dovich, we always kept the total gain $g\bar{I}L$ high enough to discriminate against the non-conjugated components in the mode approximation. In practice, this meant keeping $ln(GH) - g\bar{I}L > 5$, which resulted in choosing gains somewhat higher than those giving the maximum fidelity. (Recall Fig. 4.) Figure 6 compares the results from Ref. 5 with numerical runs made for $\theta_D = 20$ mrad (open diamonds) using $L = 20$, 40, and 75 cm, and $\theta_D = 10$ mrad (solid diamonds) using $L = 40$, 75, 200, and 300 cm. The disagreement between the theories is apparent in spite of the spread in the numerical data. In Fig. 7, these numerical results are replotted as a function of $k\theta_D/g\bar{I}$, along with additional data for $\theta_D = 5$ mrad (open squares) using $L = 200$ and 400 cm. We then see that H appears to be a function of $k\theta_D/g\bar{I}$, instead of the $k\theta_D^2/g\bar{I}$ predicted in Refs. (2-5), at least for the range of parameters studied here. The probable reason for the disagreement is that those treatments are based upon an expansion in plane waves rather than waveguide modes,[6] a point that will be explored in greater detail in Sec. V.

B. Aberrated Diverging Wave

So far, the results have been restricted to the "pure" case where the beam divergence arises entirely from the aberrator; i.e., where $\theta_D = \theta_A$. However, in most phase compensation experiments that use an optical waveguide[12,13,15–20] the aberrator is imaged onto or near the entrance face of the guide, as illustrated in Fig. 8. The light emerges from this image with a spherical (or in this case cylindrical) wavefront curvature of radius f/M, where f is the focal length of the lens, $M \equiv W_A/W$ is the magnification, and W_A is the aperature at the aberrator. This corresponds to a maximum ray divergence angle

$$\theta_F = WM/f = W_A/f \tag{20}$$

in addition to the random divergence $\theta'_A = M\theta_A$ due to the aberrator. After the light propagates within the guide a distance of order $W/(\theta_F + \theta'_A)$ beyond the image, these components should mix to produce an effective random beam divergence θ_D satisfying the condition

$$\max(\theta_F, \theta'_A) < \theta_D < \theta_F + \theta'_A. \tag{21}$$

Several numerical runs were made with the configuration shown in Fig. 8, using $\theta_F =$ mrad* and $\theta'_A = 5$ mrad ($\sim 15 \times$ diffraction limit). As in the "pure" case, a 20 cm spacing was left ... ween z_2 and the aberrator image at the waveguide entrance. Within the context of the mode approxim ...n, Eq. (15) again yielded σ values in the range 1.95-2.4, while the fidelity showed a gain depende ... similar to the one in Fig. 4, with a broad maximum around $g\bar{I}L \approx 10 - 12$ and $ln\rho > 5$ just beyon ... ax-imum.

Following the same procedure as before, we again plotted the calculated fidelity vs $k\theta_D/g\bar{I}$, where θ_D was arbitrarily chosen to be the vector sum $\theta_D \equiv (\theta_F^2 + \theta_A'^2)^{1/2} \approx 20.6$ mrad. These results (shown by the asterisks) are compared to the "pure" cases in Fig. 9. The generally good agreement, at least for $k\theta_D/g\bar{I} > 5 \times 10^3$, tends to confirm the mixing hypothesis and the important contribution of θ_F to the effective random divergence θ_D within the gain medium. The configuration modelled here is typical of most optical waveguide SBS experiments, where $\theta_F >> \theta'_A$, and thus $\theta_D \approx \theta_F$ is only weakly dependent upon θ_A. This explains why the fidelity has been found generally insensitive to the aberrator divergence in these experiments.[16]

If the aberrator is removed entirely from the cylinrically diverging beam, H follows a curve similar to Fig. 9, but it rises more rapidly with $k\theta_D/g\bar{I}$; e.g., the calculations gave $H = 20\%$ at $k\theta_D/g\bar{I} = 2900$, 86% at 5900 and 98% at 10^4. There is no reason to expect the usual analytic theories to apply in this case, however, because there is no longer a random mix of different portions of the incident beam.

IV. EFFECT OF PUMP DEPLETION

This section deals with the case where the reflectivity R is sufficient that pump depletion can become an important factor. We will examine only the configuration shown in Fig. 8, since this relates more closely to actual experiments.

Figure 10 shows the reflectivity and fidelity vs the average *incident* intensity $\bar{I}(z_2)$ for $L = 75$ cm, $\theta_F = 20$ mrad, and one member of the ensemble of aberrators with $\theta'_A = M\theta_A = 5$ mrad. The dashed line shows the fidelity that would be observed if pump depletion were ignored: i.e., if $\bar{I}(z) = \bar{I}(z_2)$ were valid throughout the length of the gain medium. It closely resembles the corresponding curve in Fig. 4, with a maximum around $g\bar{I}(z_2)L = 11$. With pump depletion, however, H continues to grow with increasing intensity and reflectivity, in agreement with the experimental results of Mays and

*Although calculations with larger divergence angles would be of interest, the additional memory storage required to ensure accuracy is somewhat beyond the present capabilities of the NRL computing system.

Lysiak.[19] This occurs because the large backscatter tends to counteract the pulling effect by selectively depleting the more intense spikes in the pump beam at $z < z_2$. An analogous effect was also seen in the focused configuration.[11] It is worth emphasizing here that if pump depletion is present, the effective average gain increment is

$$\gamma \equiv \frac{g}{L}\int_{z_1}^{z_2} \bar{I}(z)\,dz \simeq (1-R)g\bar{I}(z_2), \tag{22}$$

which can be significantly smaller than $g\bar{I}(z_2)$; e.g. at $g\bar{I}(z_2)L = 22.5$ (corresponding to $R = 41\%$), γ was calculated directly to be 13.5, in good agreement with $(1-R)g\bar{I}(z_2)L = 13.3$.

No attempt was made to plot H vs $k\theta_D/g\bar{I}(z_2)$ for the finite depletion case. (Such calculations would be costly because each point requires 10-20 iterations.) For $R \leqslant 10\%$, however, the results shown in Fig. 9 should remain a reasonable (if slightly pessimistic) approximation, while at higher reflectivities, the fidelity should at least maintain a similar functional dependence upon θ_D.

Figure 11 shows the beam profiles corresponding to the 41% reflectivity point of Fig. 10. In spite of a high conjugation fidelity ($H = 97\%$), which is evident in both the near field phase and far field intensity profiles, the near field intensity profile continues to exhibit large random inhomogeneities. An attempt was made to eliminate this problem by spatial filtering, using far field apertures of $10\theta_L$ and $4\theta_L$, where $\theta_L = 2\lambda/W_A$ is the width of the central far field spike. As seen in Fig. 12, this approach was only partly successful; thus, even the small unconjugated components in the near-axial sidelobes ($<1\%$) can significantly distort the near field.

V. DISCUSSION

The numerical calculations described in Sec. III have explored the effects of the average gain $g\bar{I}L$, gain increment $g\bar{I}$ and angular divergence θ_D upon the conjugate fidelity H in the limit of negligible pump depletion. In particular, they have studied the limitations of the mode approximation (and consequent loss of fidelity) arising from the small scale pulling effect. The resulting dependence of H upon θ_D, rather than the θ_D^2 predicted by analytic theory,[4,5] appears to be related to the discrete nature of the waveguide modes. Although a detailed treatment of the problem is beyond the scope of this paper, the result can be at least qualitatively understood by the following heuristi argument. Zel'dovich[4,5] has shown that the pulling effect arises from a summation over terms with the coefficients

$$\exp[i(K_m^2 + K_{m'}^2 - K_n^2 - K_{n'}^2)z/2k], \tag{23}$$

from which the Bragg contributions $m = n$, $m' = n'$ and $m = n'$, $m' = n$ are excluded. Here, $K_m = m\pi/W$ (where m is an integer) is the eigenvalue of the mth waveguide mode. A large degree of cancellation will occur among these terms if

$$k^{-1}(K_{\max} - K_{\min})\,\Delta K \Delta z > \pi, \tag{24}$$

where $\Delta K = \pi/W$ is the adjacent mode spacing, and $\Delta z \approx 1/g\bar{I}$ is the distance required for an appreciable secular change in the backscatter amplitude. Noting that the transverse K vector spread can be expressed as $K_{\max} - K_{\min} \approx k\theta_D$, one finally obtains the criterion

$$\theta_D/g\bar{I} > W \tag{25}$$

for the pulling effect to be small. In the simulations performed here, $W = 2$ mm; hence (25) requires $k\theta_D/gI > kW = 1.8 \times 10^4$, in good agreement with Figs. 7 and 9. Condition (25) can be rewritten in a useful form by including the gain requirement $g\bar{I}L \gtrsim 10$ to obtain

$$\theta_D > (g\bar{I}L)\ \mathrm{W/L} \gtrsim 10\mathrm{W/L}. \tag{26}$$

The second notable result in Sec. III confirms that the effective beam divergence θ_D is a combination of the aberrator divergence θ_A and the contribution from phase curvature introduced by a lens. If

a large initial phase curvature is present, one can therefore obtain good conjugation fidelity in an optical waveguide with weakly aberrated (or even unaberrated) beams, as long as the incident profile fills the aperture. It is worth noting here that the incident phase curvature also plays an important role in the focused configuration. For example, a beam of width W_A traversing an aberrator of divergence θ_A and contiguous lens of focal length f will produce small scale intensity inhomogeneities characterized by ray crossing angles $\theta \leqslant \theta_F = W_A/f$ near the focal region. Since $\theta_D \approx \theta_F$, one can usually satisfy the condition $k\theta_D^2 >> gl$ (which should be applicable to continuum modes) with only moderately aberrated beams as long as the lens F number is kept low. The important role played by phase curvature has also been noted in earlier work,[25] where the incident beam modulation was entirely in the amplitude rather than phase.

In Sec. IV, the conjugation fidelity was found to improve with pump depletion in all of the cases considered. This result is consistent with the earlier simulations in the focused configuration,[11] although the changes are less dramatic because the initial fidelities are generally higher.

Although fidelities as high as 98% were found, the near field inhomogeneities ($\geqslant$2:1 peak to valley) persisted in all cases. This behavior can be adequately explained by a simple model introduced in Ref. (11). One approximates the backscatter amplitude at the right hand side of the aberrator by a constant, plus contributions from a limited number of modes with random phase amplitudes α_ν; i.e.,

$$E_S(x) \approx R^{1/2} E_L^* \left[1 + \sum_{\nu \neq 0} \alpha_\nu \exp(i2\pi Nx/W_A)\right], \tag{27}$$

where E_L is constant within interval $-W_A/2 \leqslant x \leqslant +W_A/2$, and zero outside. This gives the near field intensity

$$|E_S(x)|^2 \approx R|E_L|^2 \left[1 + \sum_{\nu \neq 0} \alpha_\nu \exp(i2\pi Nx/W_A) + c.c.\right] \tag{28}$$

in the case of interest where $|\alpha_\nu|^2 << 1$, and the fidelity (from (9))

$$H \approx \left[1 + \sum_{\nu \neq 0} |\alpha_\nu|^2\right]^{-1}. \tag{29}$$

For N_M occupied modes of comparable RMS amplitude α_{RMS}, these expressions yield the approximate results

$$|E_S|^2_{max}/|E_S|^2_{min} \approx (1 + 2N_M^{1/2}\,\alpha_{RMS})/(1 - 2N_M^{1/2}\,\alpha_{RMS}) \tag{30}$$

$$H \approx 1 - N_M\,\alpha^2_{RMS}. \tag{31}$$

Considering the example of Fig. 11, we have $N_M\,\alpha^2_{RMS} \approx 1 - H = .03$, giving $|E_S|^2_{max}/|E_S|^2_{min} \approx 2$ in reasonable agreement with the near field structure shown in the figure. It is interesting to note that even for $H = 99\%$, this model predicts near field intensity variations up to 1.5:1.

ACKNOWLEDGMENTS

The author gratefully acknowledges the valuable discussions and suggestions of Harvey Brock and Peter Ulrich. This work was supported jointly by the Office of Naval Research and the U.S. Department of Energy.

REFERENCES

1. R.W. Hellwarth, "Optical beam phase conjugation by stimulated backscattering," Opt. Eng. **21**, 257 (1982), and references therein.

2. V.G. Sidorovich, "Theory of the Brillouin Mirror," Zh. Tekh. Fiz. **46**, 2168 (1976) [Translation: Sov. Phys. Tech. Phys. **21**, 1270 (1976)].

3. I.M. Bel'dyugin M.G. Galushkin, E.M. Zemskov, and V.I. Mandrosov, "Complex conjugation of fields in stimulated Brillouin scattering," Kvant. Elektron 3, 2467 (1976) [Translation: Sov. JQE 6, 1349 (1976)].

4. B. Ya. Zel'dovich and V.V. Shkunov, "Limits of existence of wavefront reversal in stimulated light scattering," Kvant. Elektron. 5, 36 (1978) [Translation: Sov. JQE 8, 15 (1978)].

5. B. Ya. Zel'dovich and T.V. Yakovleva, "Calculations of the accuracy of wavefront reversal utilizing pump radiation with one-dimensional transverse modulation," Kvant. Elektron. 8, 314 (1981) [Translation: Sov. JQE 11, 186 (1981)].

6. R.W. Hellwarth, "Theory of phase conjugation by stimulated scattering in a waveguide," J. Opt. Soc. Am. 68, 1050 (1978).

7. R.H. Lehmberg, "Theory of optical ray retracing in laser-plasma backscatter," Phys. Rev. Lett. 41, 863 (1978).

8. N.B. Baranova, B. Ya. Zel'dovich, and V.V. Shkunov, "Wavefront reversal in stimulated light scattering in a focused spatially inhomogeneous pump beam," Kvant.Elektron. 5, 973 (1978) [Translation: Sov. JQE 8, 559 (1978)].

9. N.B. Baranova and B. Ya. Zel'dovich, "Wavefront reversal of focused beams (theory of stimulated Brillouin backscattering)," Kvant. Elektron. 7, 973 (1980) [Translation: Sov. JQE 10, 555 (1980].

10. G.G. Kochemasov and V.D. Nikolaev, "Investigation of the spatial characteristics of Stokes radiation in stimulated scattering under saturation conditions," Kvant. Elektron. 6, 1960 (1979) [Translation: Sov. JQE 9, 1155 (1979)].

11. R.H. Lehmberg, "Numerical study of phase conjugation in stimulated backscatter with pump depletion," Optics Comm. (in press).

12. B. Ya. Zel'dovich, V.I. Popovichev, V.V. Ragul'skii, and F.S. Faizullov, "Connection between the wave fronts of the reflected and exciting light in stimulated Mandel'shtam-Brillouin scattering," Pis. Zh. ETF 15, 160 (1972) [Translation: JETP Lett. 15, 109 (1972)].

13. O. Yu. Nosach, V.I. Popovichev, V.V. Ragul'skii and F.S. Faizullov, "Cancellation of Phase distortions in an amplifying medium with a Brillouin Mirror," ZhETF Pis. Red. 16, 617 (1972) [Translation: Sov. Phys. JETP Lett. 16, 435 (1972)].

14. V.N. Blashchuk, et al., "Wavefront inversion in stimulated scattering of focused light beams," Pis. Zh. Tekh. Fiz. 3, 211 (1977) [Translation: Sov. Tech. Phys. Lett. 3, 83 (1977)].

15. V. Wang and C.R. Guiliano, "Correction of phase aberrations via Stimulated Brillouin scattering," Opt. Lett. 2, 4 (1978).

16. C.R. Guiliano, R.W. Hellwarth, R.K. Jain, R.C. Lind, T.R. O'Meara, S.M. Wandzura, and V. Wang, "*Correction of Phase Distortion by Nonlinear Optical Techniques*," Hughes Research Laboratories Interim Technical Report for period 15 July 1977 - 30 September 1978 (March 1979).

17. N.G. Basov, V.F. Efimkov, I.G. Zubarev, A.V. Kotov, A.B. Mironov, S.I. Mikhailov, and M.G. Smirnov, "Influence of certain radiation parameters on wavefront reversal of a pump wave in a Brillouin mirror," Kvant. Elektron. 6, 765 (1979) [Translation: Sov. JQE 9, 455 (1979)].

18. R. Mays, Jr. and R.J. Lysiak, "Phase conjugated wavefronts by stimulated Brillouin and Raman scattering," Optics Comm. **31**, 89 (1979).

19. R. Mays, Jr. and R.J. Lysiak, "Observations of wavefront reproduction by stimulated Brillouin and Raman scattering as a function of pump power and waveguide dimensions," Optics Comm. **32**, 334 (1980).

20. N.F. Pilipetskii, V.I. Popovichev, and V.V. Ragul'skii, "Comparison of the amplification coefficients of conjugate and nonconjugate waves in stimulated light scattering," Optics Comm. **40**, 73 (1981).

21. M.C. Gower and R.G. Caro, "KrF laser with a phase-conjugate Brillouin mirror," Opt. Lett. **7**, 162 (1982).

22. V.I. Bespalov, A.A. Betin, and G.A. Pasmanik, "Reconstruction effects in stimulated scattering," Pis. Zh. Tekh. Fiz. **3**, 215 (1977) [Translation: Sov. Tech. Phys. Lett. **3**, 85 (1977)].

23. A.I. Sokolovskyaya, G.L. Blekhovskikh, and A.D. Kudryavtseva, "Light beam wavefront reconstruction and real volume image reconstruction of the object in stimulated Raman scattering," Optics Comm. **24**, 74 (1978).

24. M. Slatkine, I.J. Bigio, B.J. Feldman, and R.A. Fisher, "Efficient phase conjugation of an ultraviolet XeF laser beam by stimulated Brillouin scattering," Opt. Lett. **7**, 108 (1982).

25. R.H. Lehmberg and K.A. Holder, "Numerical study of optical ray retracing in laser-plasma backscatter," Phys. Rev. **22**, 2156 (1980).

26. J.A. Fleck, Jr., J.R. Morris, and M.D. Feit, "Time dependent propagation of high energy laser beams through the atmosphere," Appl. Phys. (Springer) **10**, 129 (1976); **14**, 99 (1977).

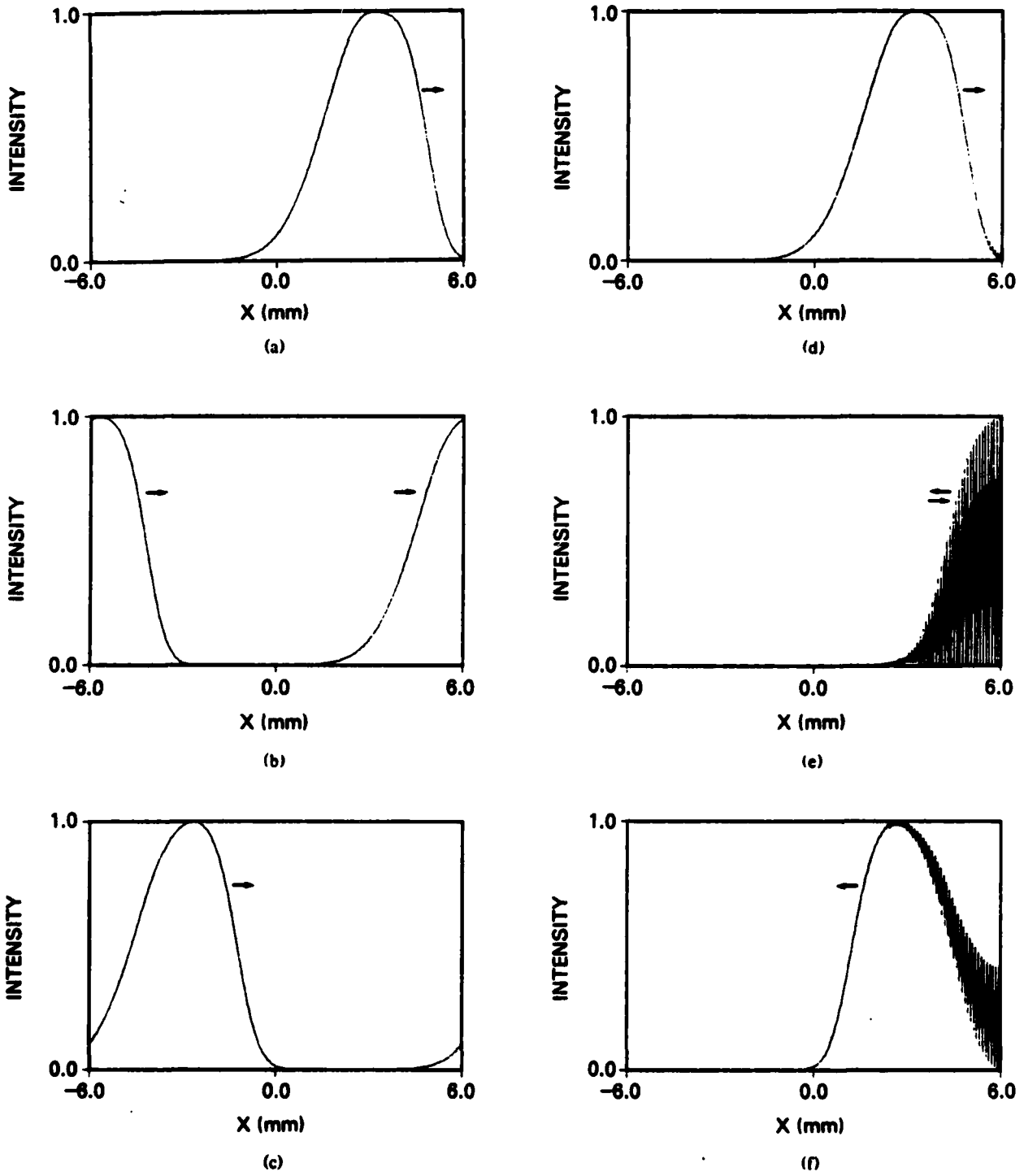

Fig. 1 — Intensity profiles of a nonaxially propagating wave in a linear medium, calculated with the conventional DFT (*a–c*), and the waveguide modes (*d–f*)

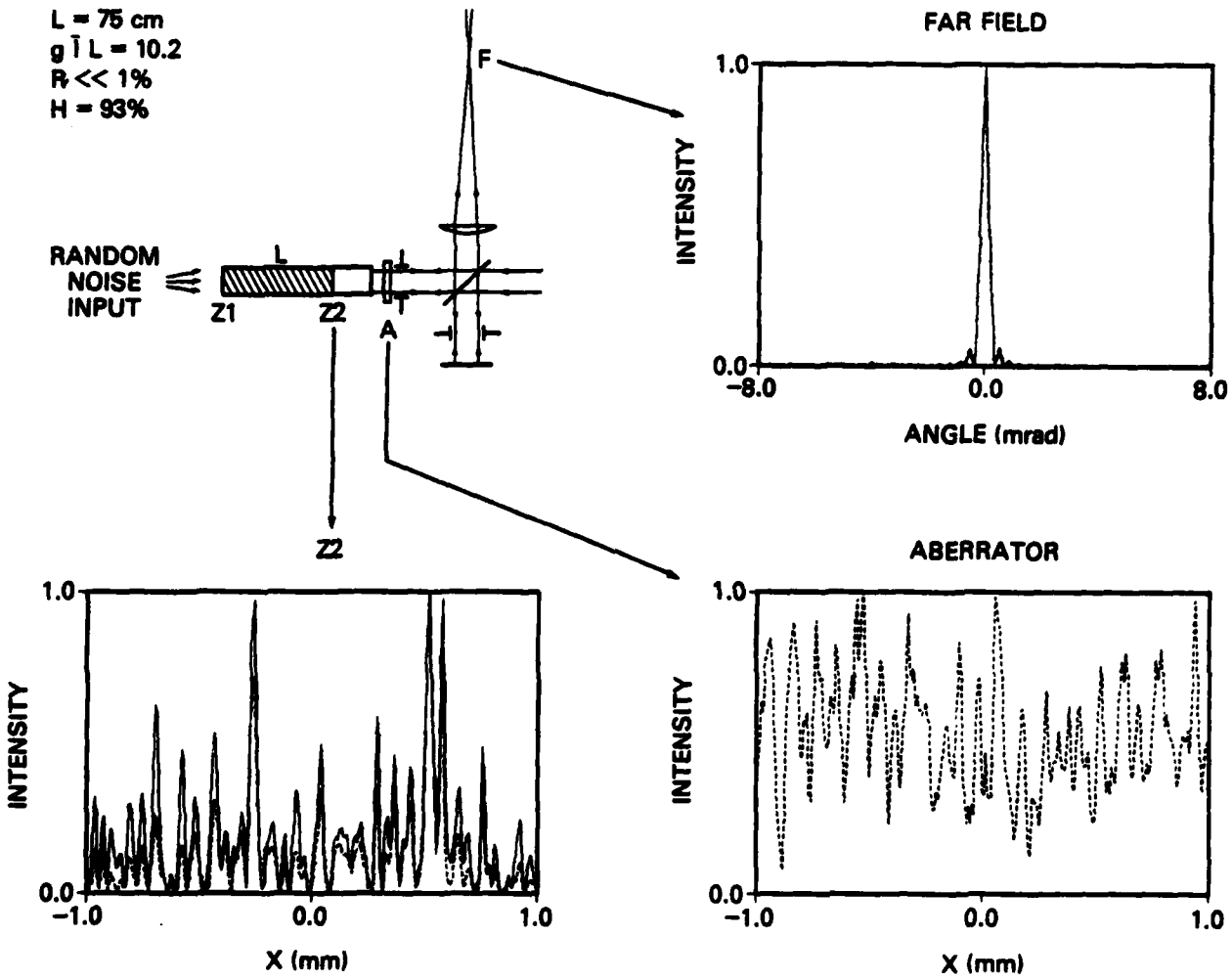

Fig. 2 — Simulation of SBS wavefront conjugation in an optical waveguide with a 75 cm gain length, showing intensity profiles of the incident light (solid lines) and backscatter (dashed lines) with negligible pump depletion. (The incident intensity is uniform across the aberrator.)

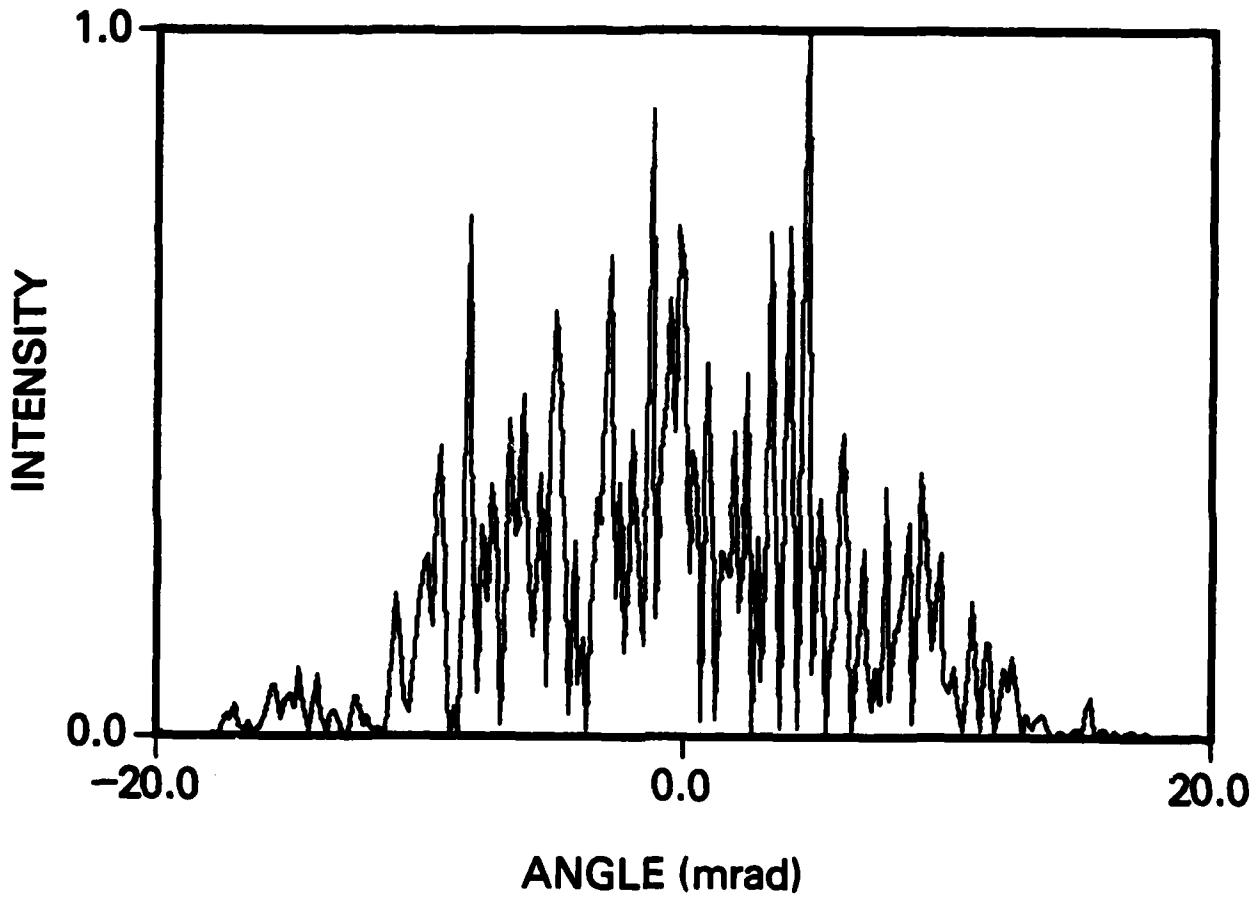

Fig. 3 — Far field intensity profile of the incident light after traversing an aberrator of 20 mrad (full $1/e$) angular divergence

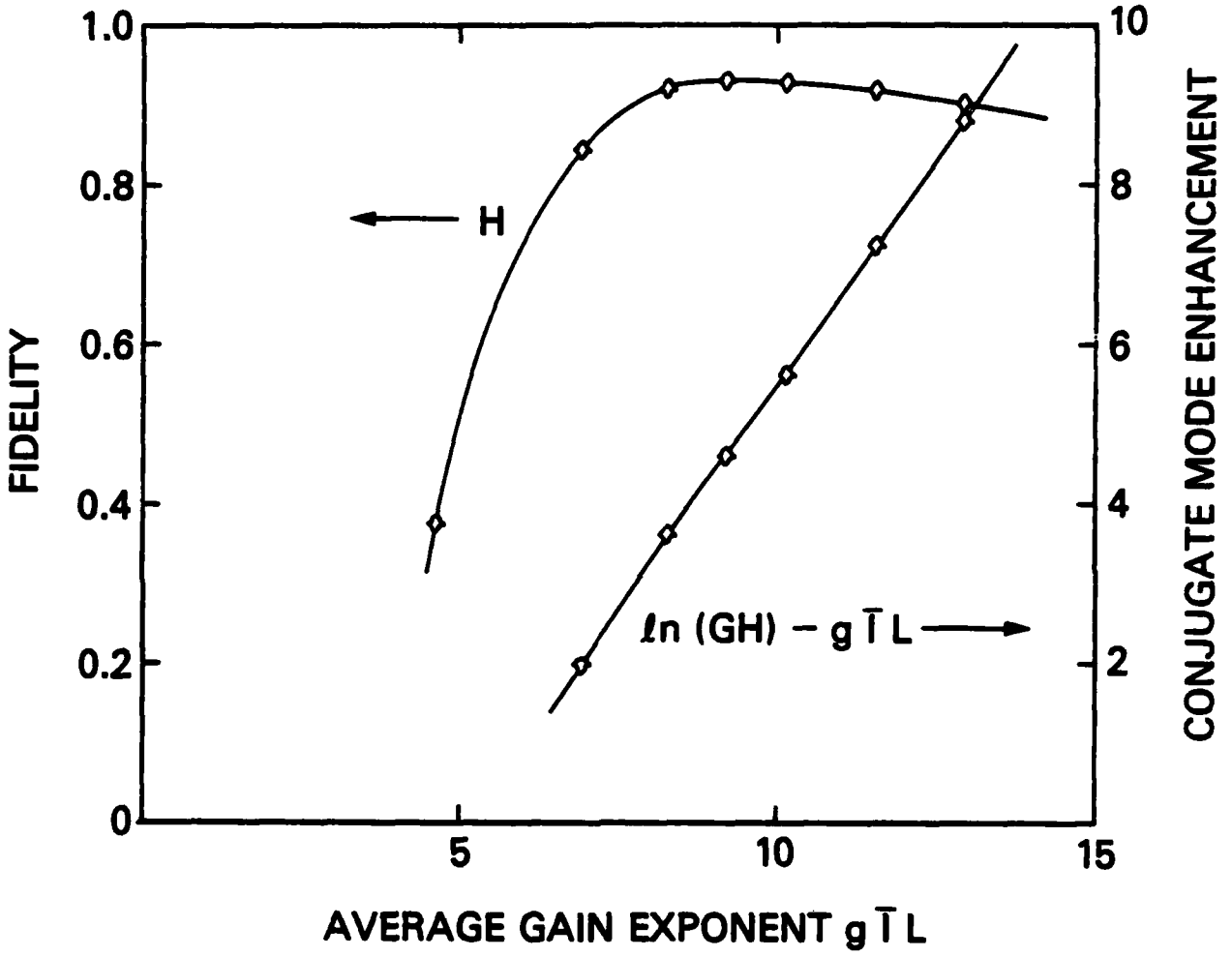

Fig. 4 — Conjugation fidelity H and conjugate mode enhancement factor $\ln\rho$ [Eqs. (16) and (19)] vs average (amplitude) gain exponent for the same aberrator and gain length used in Fig. 2

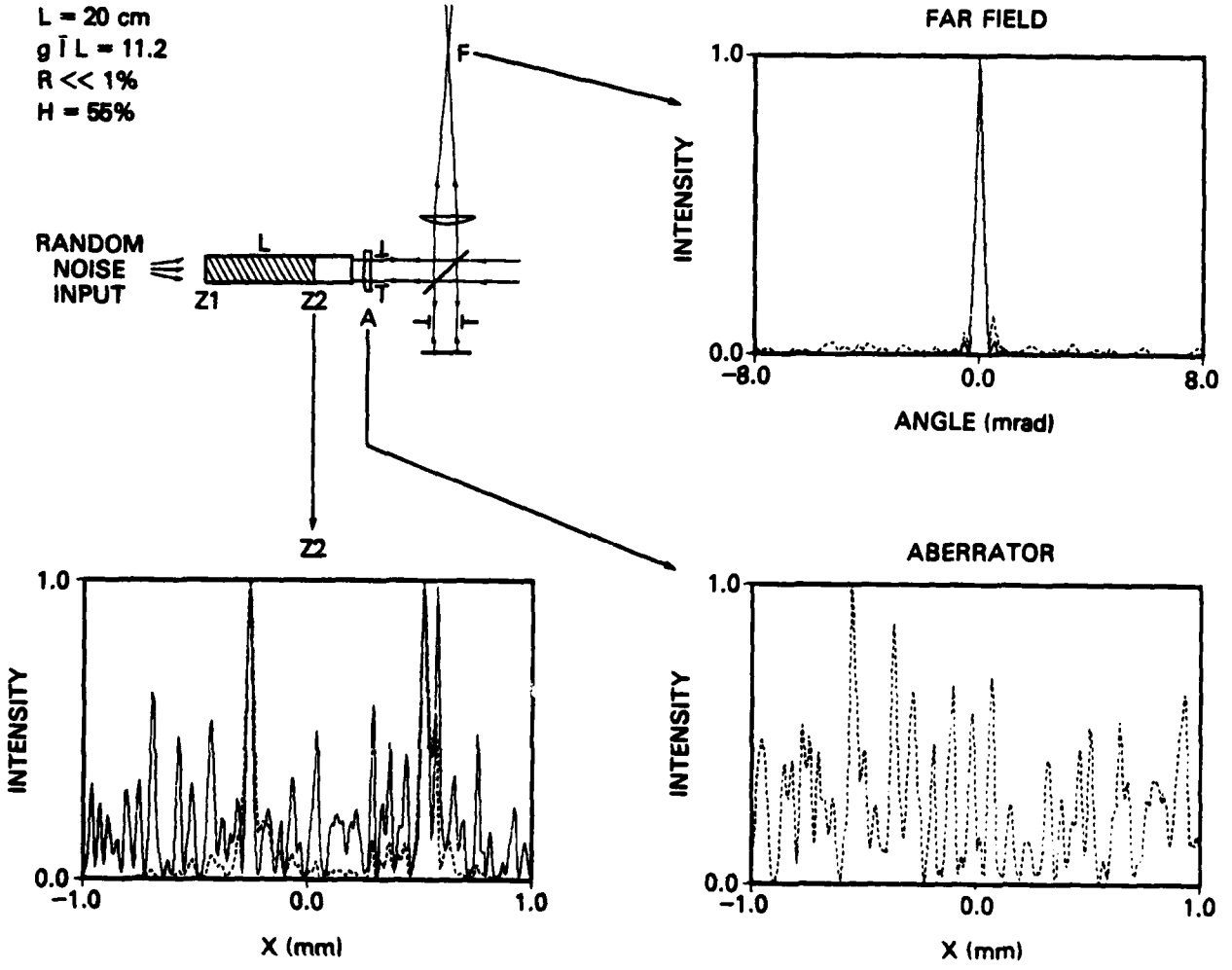

Fig. 5 — Same as Fig. 2, except for a shorter gain length (L = 20 cm)

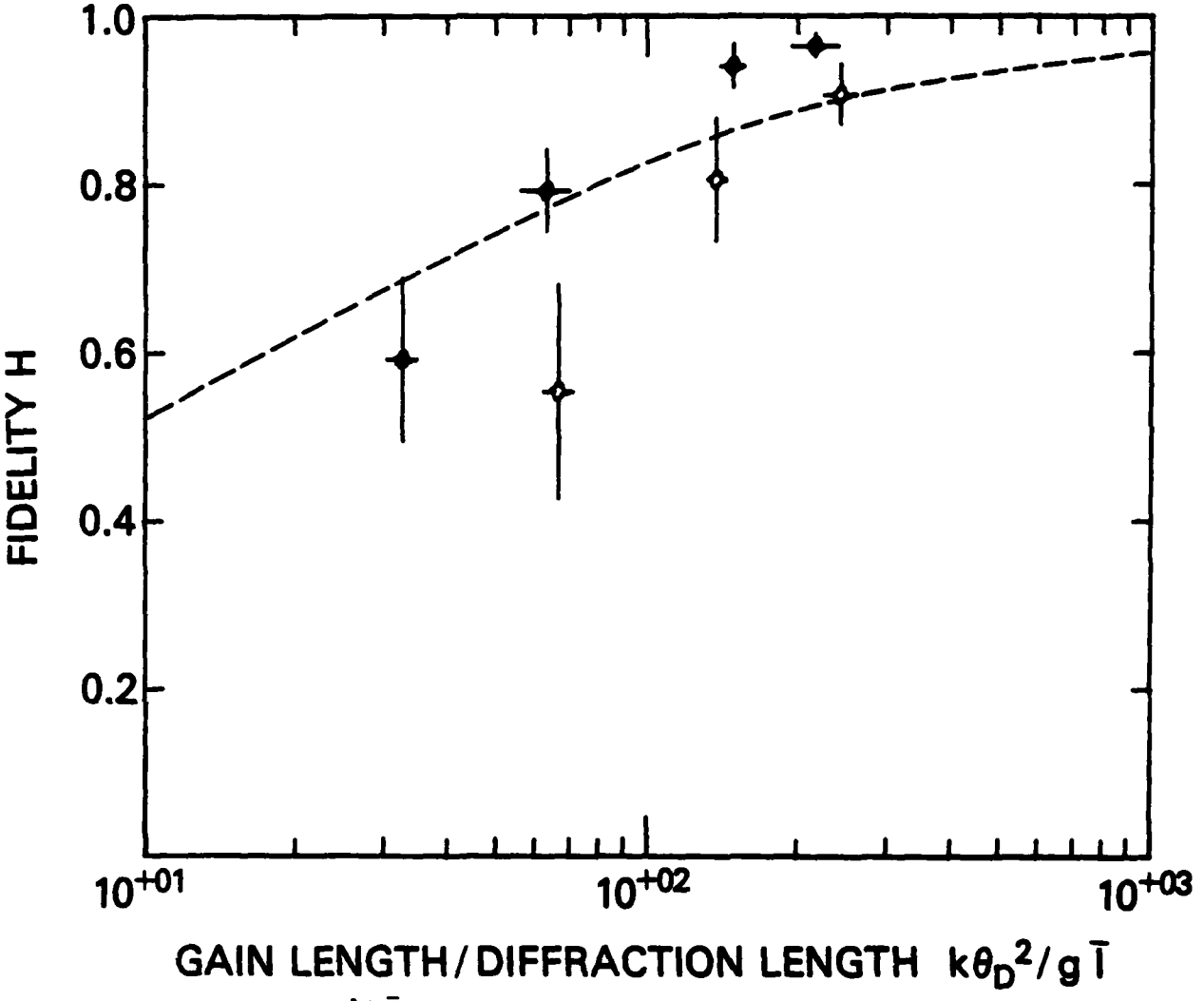

Fig. 6 — Conjugation fidelity vs $k\theta_D^2/g\bar{l}$. as calculated from Ref. 5 (dashed curve) and simulations with aberrators of 10 mrad (solid diamonds) and 20 mrad (open diamonds) far field divergence. Each point shows the average and mean deviation of five simulations using independent aberrators.

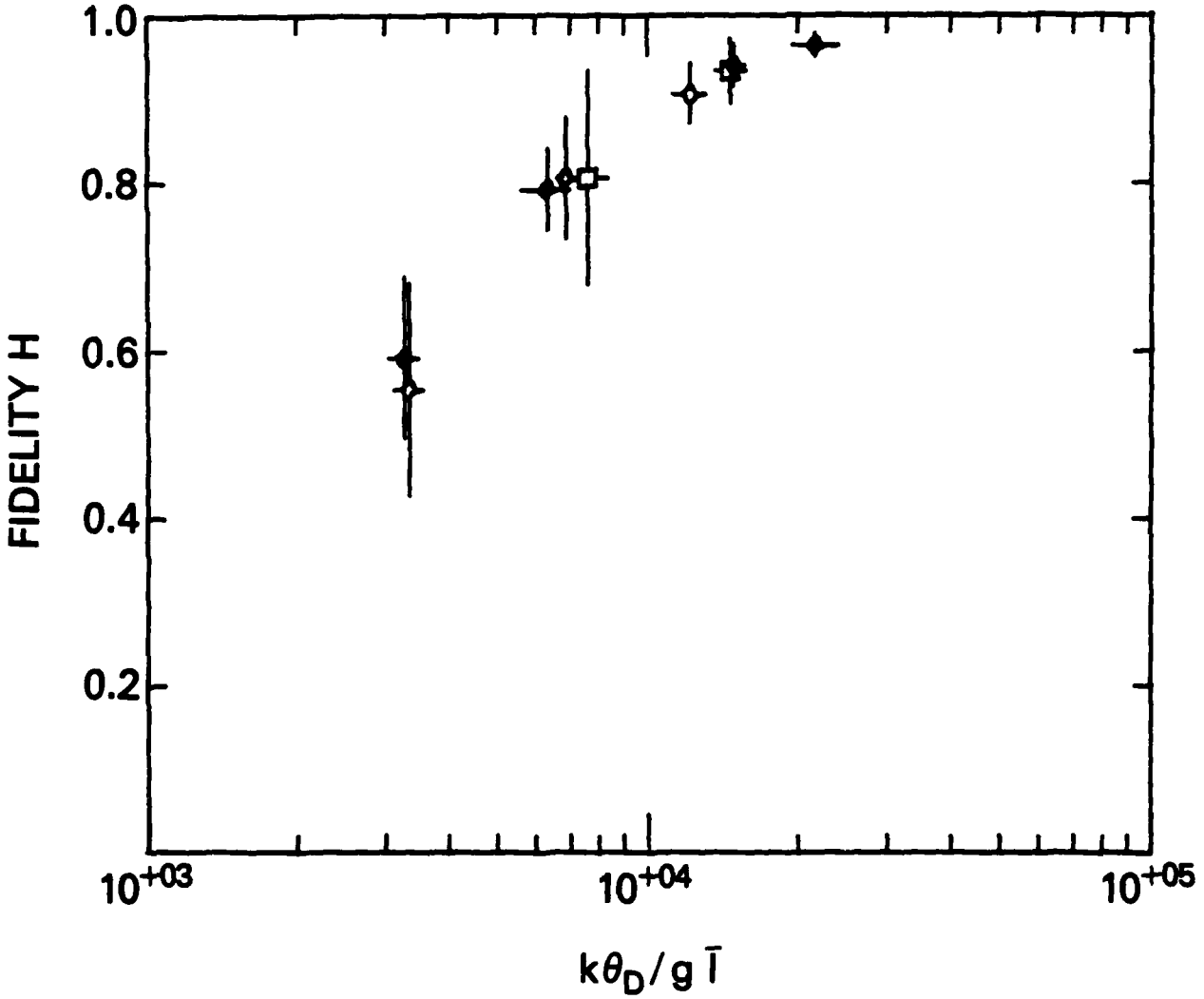

Fig. 7 — Conjugation fidelity vs $k\theta_D/g\bar{l}$ from simulations with aberrators of 5 mrad (open squares), 10 mrad (solid diamonds) and 20 mrad (open diamonds) far field divergence

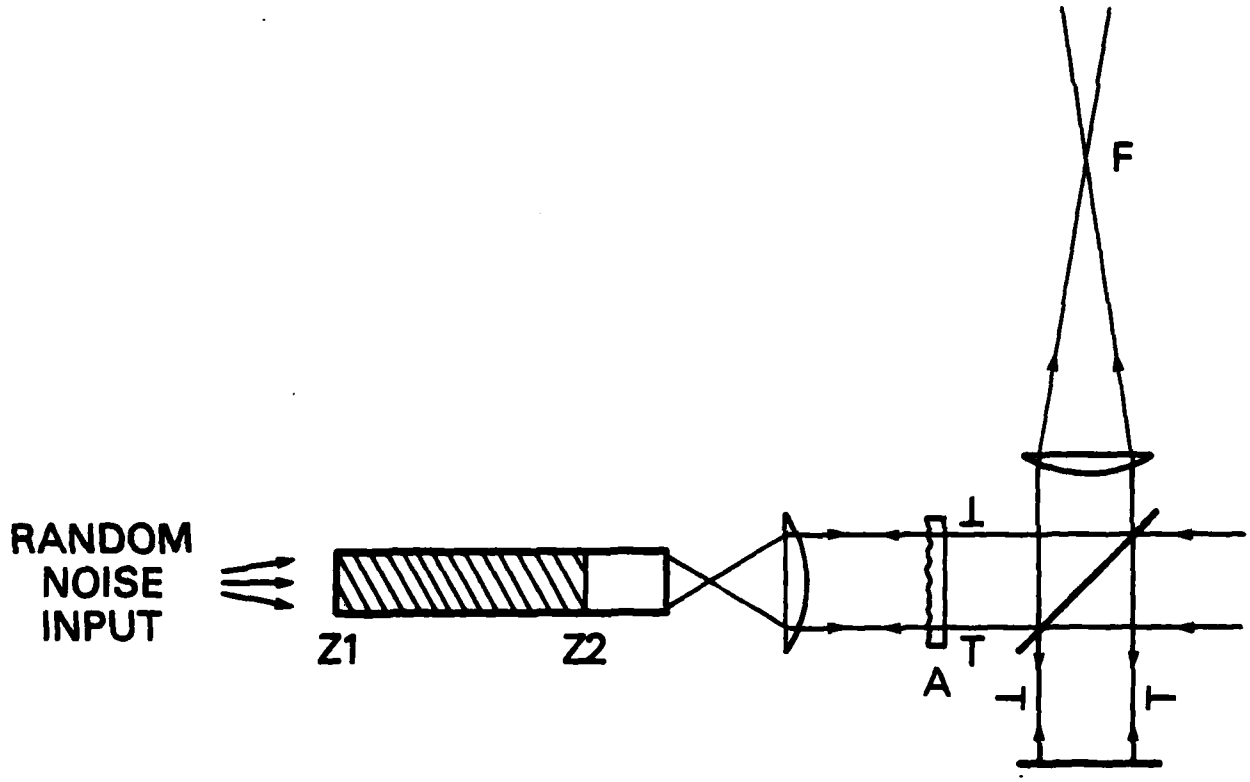

Fig. 8 — SBS wavefront conjugation geometry, where aberrator A is imaged onto the entrance face of the optical waveguide

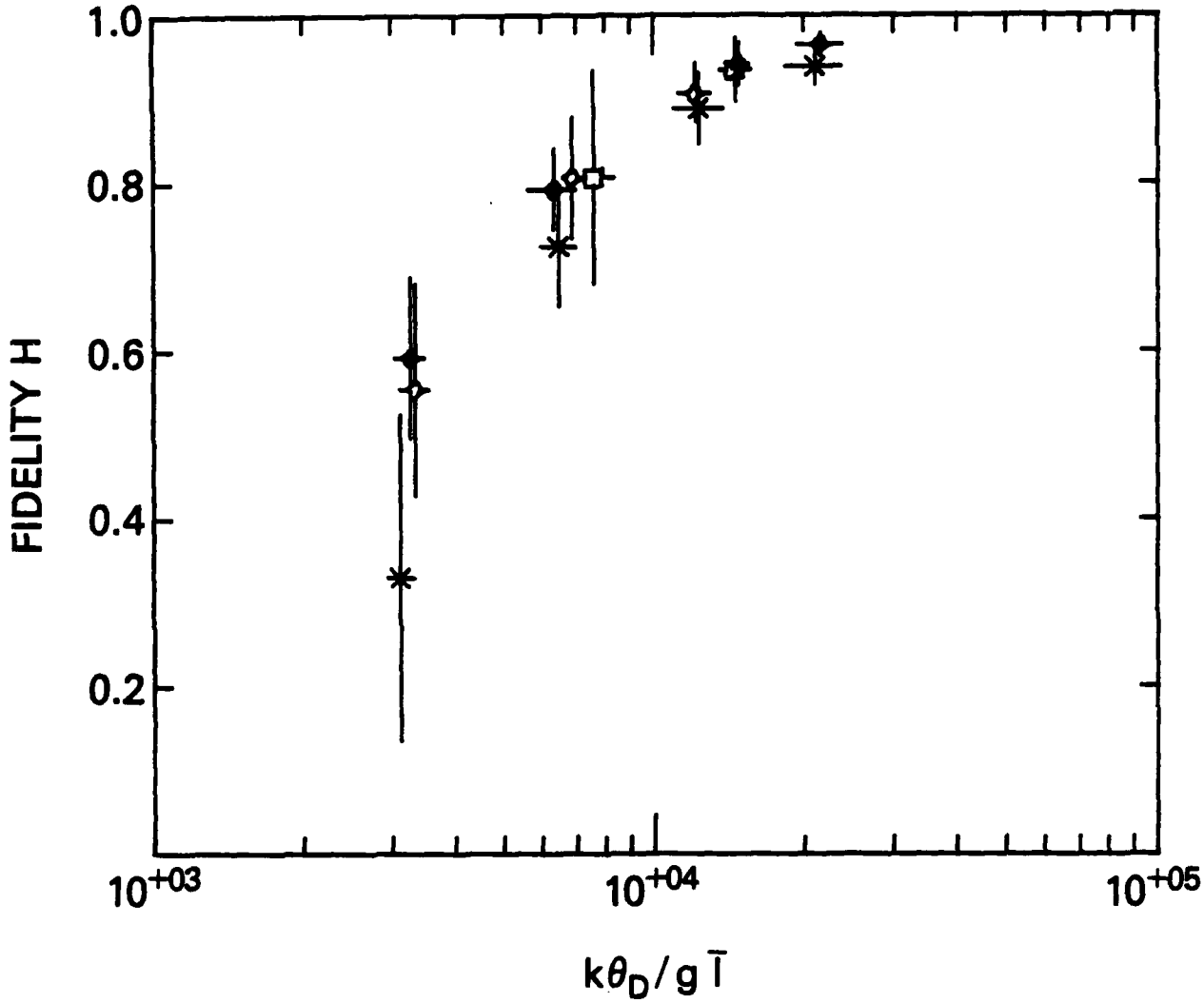

Fig. 9 — Comparison between the fidelity vs $k\theta_D/g\bar{I}$ data of Fig. 7 and simulations of the geometry shown in Fig. 8 (asterisks), using θ_D = 20.6 mrad

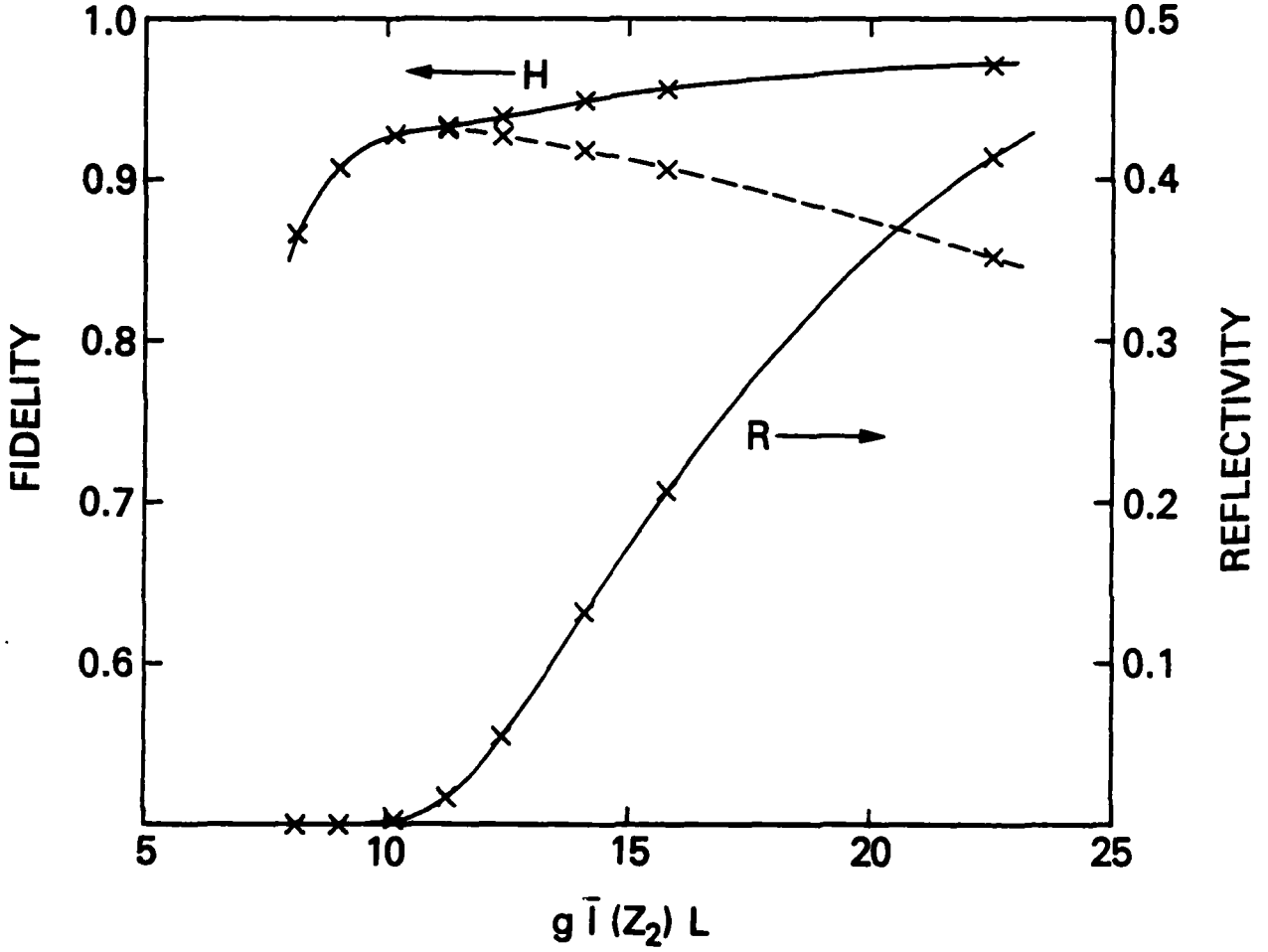

Fig. 10 — Conjugation fidelity H and reflectivity R vs incident intensity from simulations of the model shown in Fig. 8 (L = 75 cm, θ_D = 5 mrad, θ_F = 20 mrad). The dashed line shows the fidelity in the absence of pump depletion.

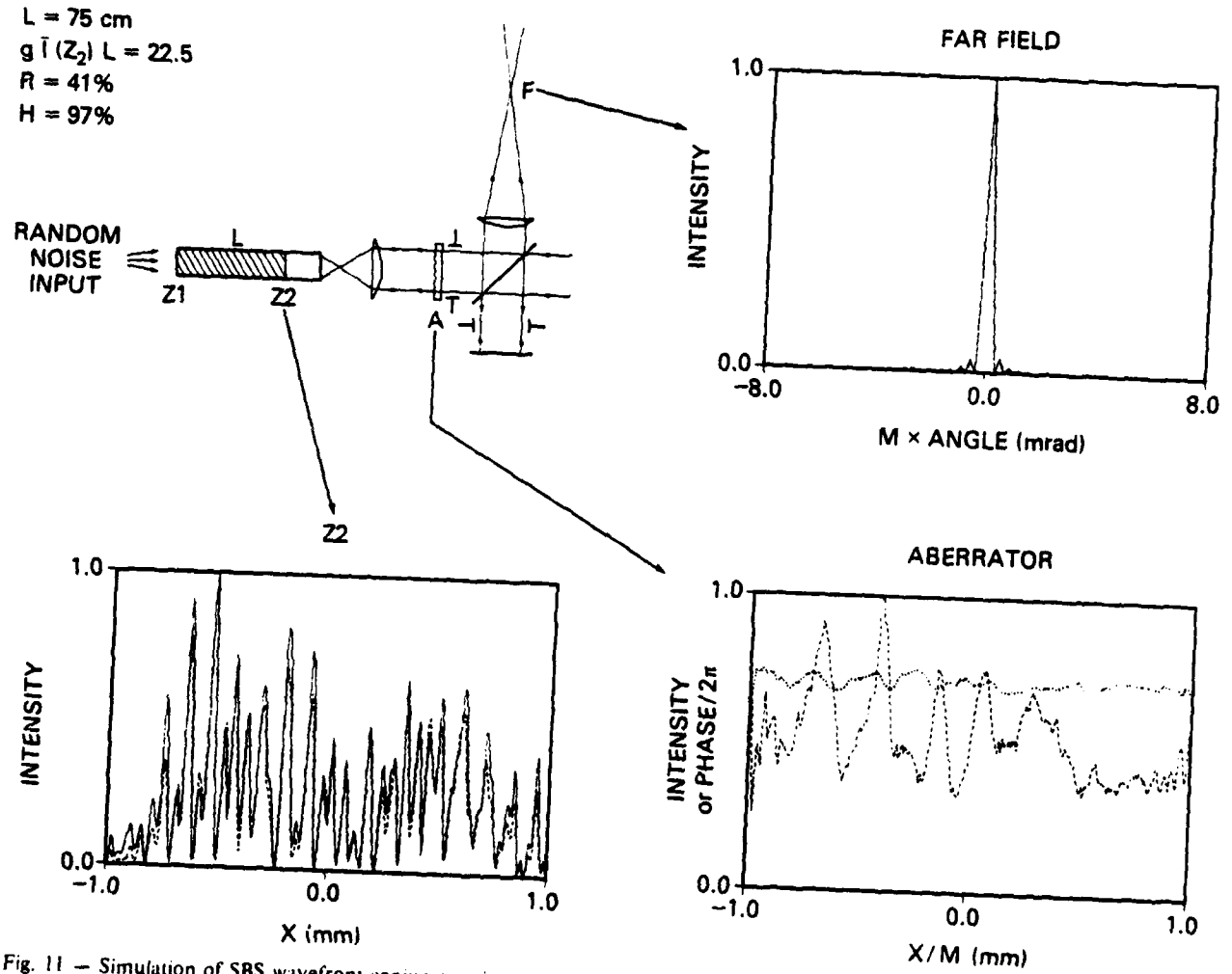

Fig. 11 — Simulation of SBS wavefront conjugation in an optical waveguide with pump depletion (corresponding to the $R = 41\%$ point of Fig. 10). The intensity profiles have the same meaning as in Figs. 2 and 5. The dotted line in the near field plot is the phase of the backscattered field after it traverses the aberrator.

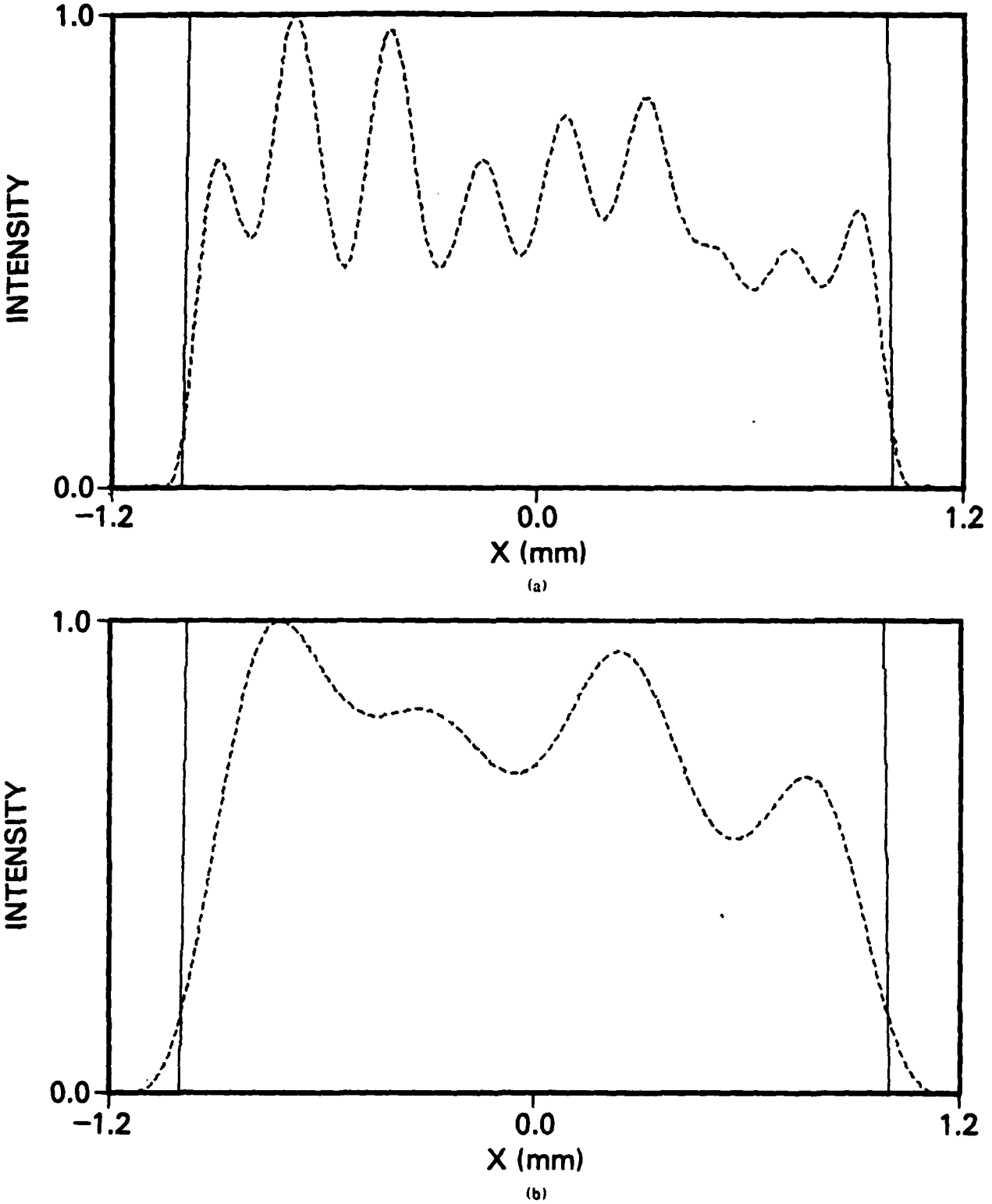

Fig. 12 — Comparisons between the "top hat" incident pump profile and an image of the backscatter at the aberrator, using spatial filtering with far field apertures of 10 × diffraction limit (a) and 4 × diffration limit (b)


2-8
DT